

Metalloenzymes

N₂O Reduction by the μ_4 -Sulfide-Bridged Tetranuclear Cu_Z Cluster Active Site**

Peng Chen, Serge I. Gorelsky, Somdatta Ghosh, and Edward I. Solomon*

Keywords:

bioinorganic chemistry · copper · electronic structure · metalloenzymes · structure–activity relationships

Nitrous oxide (N₂O) reduction is a chemical challenge both in the selective oxidation of organic substrates by N₂O and in the removal of N₂O as a green-house gas. The reduction of N₂O is thermodynamically favorable but kinetically inert, and requires activating transition-metal centers. In biological systems, N₂O reduction is the last step in the denitrification process of the bacterial nitrogen cycle and is accomplished by the enzyme nitrous oxide reductase, whose active site consists of a μ_4 -sulfide-bridged tetranuclear Cu_Z cluster which has many unusual spectroscopic features. Recent studies have developed a detailed electronic-structure description of the resting Cu_Z cluster, determined its catalytically relevant state, and provided insight into the role of this tetranuclear copper cluster in N₂O activation and reduction.

1. Introduction

Selective oxidation of organic substrates is a significant challenge.^[1] Reagents energetically capable of performing useful oxidations are often so reactive that they offer no substrate selectivity; others produce byproducts that lead to undesirable side reactions. A potentially attractive oxo-transfer reagent to oxidize organic substrates is nitrous oxide (N₂O + 2H⁺ + 2e⁻ → N₂ + H₂O, E° = 1.76 V),^[2] which provides a clean reaction since the sole byproduct is N₂. However, N₂O is a kinetically inert molecule, which is reflected in the

approximately 59 kcal mol⁻¹ activation barrier for its thermal decomposition (a unimolecular, spin-forbidden process).^[3] Reduction of N₂O in homogeneous systems normally requires transition metals, such as Ti, V, Ni, Zr, Ru, Hf,^[4–9] as activation centers, where the required two electrons are either derived

from the metal centers, which results in terminal^[10,11] or bridged^[4] metal-oxide products, or from the ligands through insertion of the oxygen atom into the metal–ligand bond.^[5–7,12] To date, none of the reported metal/N₂O complexes has been structurally determined crystallographically. The N₂O unit in the [(NH₃)₅Ru(N₂O)]²⁺ complex has been found from spectroscopy to coordinate to the ruthenium atom in a linear end-on mode by its terminal nitrogen atom.^[13] Additional terminal oxygen coordination to metal sites has also been implicated in the formation of the {Ru(N₂O)Ru} dimer^[10,14] and has been spectroscopically identified in N₂O adsorption on α -Cr₂O₃.^[15]

The reduction of N₂O in biological systems is accomplished by the multicopper-center containing enzyme nitrous oxide reductase (N₂OR). This reaction is the last step of the denitrification process, where the denitrifying organisms utilize oxidized forms of nitrogen in place of oxygen as the terminal electron acceptors for anaerobic respiration (Figure 1) that is coupled to ATP synthesis.^[16] The reduction of N₂O is also environmentally important because N₂O is a green-house gas (third only to CO₂ and CH₄) and largely generated from artificial fertilizers used in farming and from the burning of fossil fuels.^[3,16] The enzyme N₂OR contains two types of copper active sites, Cu_A and Cu_Z.^[16–18] The Cu_A center is a well-characterized electron-transfer site with two copper atoms bridged by two cysteine ligands.^[19,20] The structure of

[*] P. Chen, Dr. S. I. Gorelsky, S. Ghosh, Prof. Dr. E. I. Solomon
Department of Chemistry
Stanford University
Stanford, California 94305 (USA)
Fax: (+1) 650-725-0259
E-mail: Edward.Solomon@Stanford.Edu

[**] This research is supported by NIH grant DK-31450 (E.I.S.). The S K-edge data were collected by Dr. S. DeBeer George (Stanford Synchrotron Radiation Laboratory). We thank Profs. I. Moura (Portugal), D. Dooley (Montana State University), K. Hodgson and B. Hedman (Stanford Synchrotron Radiation Laboratory), and W. E. Antholine (Wisconsin Medical College) for collaborations on different parts of this research. P.C. was supported by a Gerhard Casper Stanford Graduate Fellowship and a Franklin Veatch Memorial Fellowship. S.I.G. has been supported by a NSERC (Ottawa) postdoctoral fellowship.

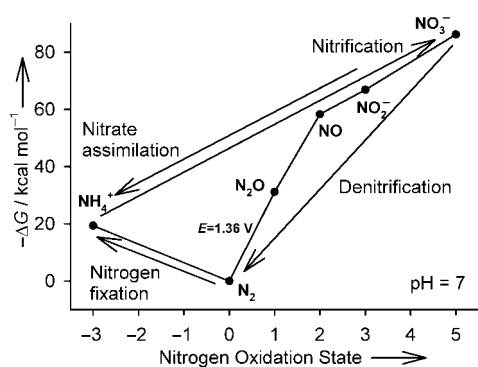


Figure 1. Bacterial nitrogen cycle and its thermochemistry (aqueous solution at pH 7). The values of ΔG (ox + $n e^- \rightarrow$ red) refer to N₂ as standard (zero) but are quoted per mol of N atoms.

the catalytic Cu_Z site, however, was elusive and was originally assigned as a binuclear copper center based on some initial spectroscopic results.^[21,22] A low-resolution crystal structure (2.4 Å) was later solved for N₂OR from *Pseudomonas nautica* (*Pn*),^[23] and indicated that the Cu_Z center has a strikingly new structural motif composed of a bridged tetranuclear copper cluster and is located in the N-terminal domain in each subunit of the dimeric protein, while the Cu_A center is located in the C-terminal domain of each subunit. The neighboring Cu_A and Cu_Z centers are from different subunits in the dimeric protein (Figure 2). Quantitative elemental analysis combined with spectroscopic arguments soon indicated that the Cu_Z center is in fact a μ_4 -sulfide bridged tetranuclear

copper cluster.^[24] This was later confirmed by the high-resolution crystal structure of N₂OR from *Paracoccus denitrificans* (*Pd*) (1.6 Å), and the original *Pn* N₂OR structure was then revised.^[25,26]

The Cu₄S core of the Cu_Z structure has approximate C_s symmetry with Cu_I-S-Cu_{II} defining the mirror plane (see Figure 2). The Cu_I-S-Cu_{II} angle is approximately 160°, and the other Cu-S-Cu angles are close to orthogonal. All the Cu-S bond lengths are approximately the same, about 2.3 Å. However, the Cu-Cu separations are very different, with the three copper centers, Cu_{II}, Cu_{III}, Cu_{IV} (Figure 2), closer to each other and Cu_I more distant (Cu_I-Cu_{III}/Cu_I-Cu_{IV} ≈ 3.4 Å, Cu_{II}-Cu_{III}/Cu_{II}-Cu_{IV} ≈ 2.6 Å, Cu_{III}-Cu_{IV} ≈ 2.9 Å). The whole {Cu₄S} cluster is coordinated to the protein backbone by seven histidine ligands, and there is an additional ligand L at the Cu_I/Cu_{IV} edge. This Cu_I/Cu_{IV} edge is believed to be the substrate binding site.^[23] To date the exact nature of this ligand (O²⁻, OH⁻, H₂O) is unclear from the crystal-structure studies.

Much spectroscopic data have been published on the resting Cu_Z center,^[27] including its absorption spectrum (Figure 3a, solid line) which shows an intense charge-transfer (CT) band at about 640 nm (≈ 15650 cm⁻¹), and the low-temperature magnetic circular dichroism (MCD) spectrum (Figure 3a, broken line) which has an intense feature in this 640 nm region.^[21,22,24,28] The EPR spectrum of resting Cu_Z has also been reported, it exhibits a very small g_{||} value and complicated hyperfine-coupling pattern.^[18,21,28] However, because of the lack of accurate quantification of the number of copper atoms in the enzyme, their oxidation states, and



Peng Chen received his B.S. from Nanjing University, China in 1997. After spending a year at University of California at San Diego with Prof. Yitzhak Tor, he moved to Stanford University to work with Prof. Edward I. Solomon. There he did his Ph.D. on the electronic structure studies of biologically relevant Cu sites involved in O₂ and N₂O activation. He was supported by a Gerhard Casper Stanford Graduate Fellowship and a Franklin Veatch Memorial Fellowship. He recently started his postdoctoral research with Prof. Sunney Xie at Harvard University.



Somdatta Ghosh was born in Kolkata, India. She received her B.S. degree from Presidency College, Calcutta University, and M.S. degree from the Indian Institute of Technology, Kanpur. She moved to Stanford University as a graduate student in 2002, and joined the research group of Prof. Edward I. Solomon. Her research focuses on spectroscopic, kinetic, and computational studies aimed at elucidating the mechanism of N₂O reduction and substrate oxygenation by copper containing enzymes.



Serge Gorelsky received his B.S. and M.S. from Moscow State University. He completed his Ph.D. under the supervision of Prof. A. Barry P. Lever at York University, Toronto, on electronic spectroscopy of ruthenium complexes. In 2002, he joined Prof. Edward I. Solomon's group at Stanford University as an NSERC Postdoctoral Fellow. His research focuses on electronic-structure and spectroscopic studies of copper-containing proteins. He is a recipient of Governor General of Canada's Gold Medal for academic excellence (2002).



Edward I. Solomon grew up in North Miami Beach, Florida, received his Ph.D. from Princeton University (with D. S. McClure), and was a postdoctoral fellow at the H. C. Ørsted Institute (with C. J. Ballhausen) and then at Caltech (with H. B. Gray). He was a professor at MIT until 1982. He then moved to Stanford University where he is now a Monroe E. Spaght Professor of Humanities and Sciences. His research is in the fields of physical-inorganic and bioinorganic chemistry with emphasis on the elucidation of electronic structures and their contributions to the physical properties and reactivity of transition-metal complexes.

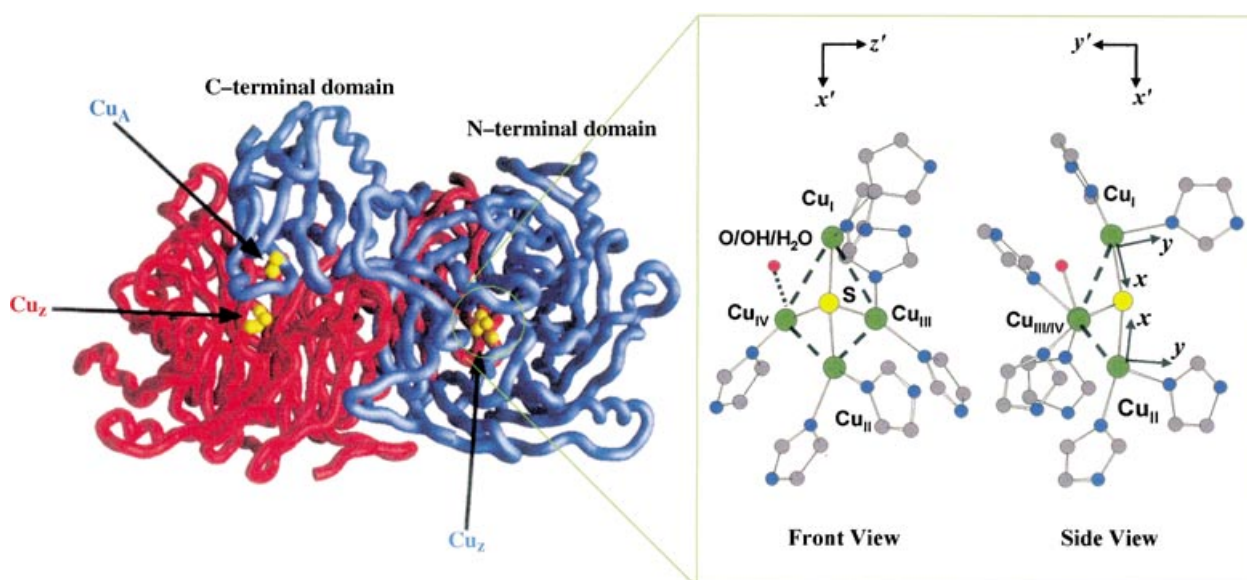


Figure 2. Crystal structure of the Cu_2 site from *Pn*. The two subunits in the homodimeric protein are indicated in red and blue. The Cu_4S cluster has approximate C_s symmetry with $\text{Cu}_I\text{-S-Cu}_{III}$ defining the mirror plane. $r(\text{Cu-S}) \approx 2.3 \text{ \AA}$, $r(\text{Cu}_I\text{-Cu}_{II})$ and $r(\text{Cu}_I\text{-Cu}_{IV}) \approx 3.4 \text{ \AA}$, $r(\text{Cu}_{II}\text{-Cu}_{III})$ and $r(\text{Cu}_{II}\text{-Cu}_{IV}) \approx 2.6 \text{ \AA}$, $r(\text{Cu}_{III}\text{-Cu}_{IV}) \approx 2.9 \text{ \AA}$; $\text{Cu}_I\text{-S-Cu}_{II} \approx 160^\circ$, all other Cu-S-Cu angles are close to 90° . The water-derived ligand L (O^{2-} , OH^- , H_2O) is weakly bound according to the higher resolution structure of *Pd* (1.6 \AA resolution) with $r(\text{Cu}_{IV}\text{-O}) \approx 2.6 \text{ \AA}$ and $r(\text{Cu}_I\text{-O}) \approx 2.8 \text{ \AA}$, however its nature has not been assigned. Molecular (x', y', z') and local (x, y, z) coordinate systems are indicated, which are used for labeling orbitals.

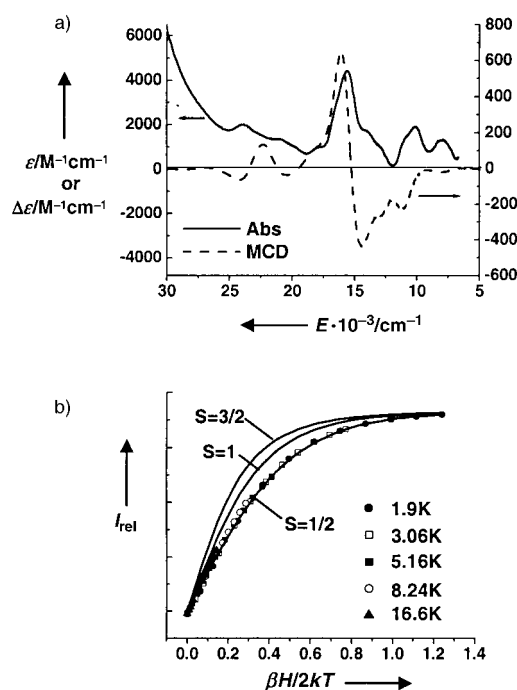


Figure 3. a) absorption spectrum of resting Cu_2 from *Pn* N_2OR at 10 K and the corresponding 7 T MCD spectrum at 5 K. b) VTVH saturation MCD (points) at 620 nm of resting Cu_2 along with simulated saturation curves (solid lines).

structural information, a reasonable understanding of these spectral features and the enzymatic mechanism had not been possible. Herein, we focus on our recent efforts to understand these spectroscopic features and develop an electronic-structure description of the Cu_2 site of the N_2OR enzyme.^[29–31]

Insight into the contribution of the electronic structure to N_2O reduction and the possible mechanism for this reaction by the Cu_2 center are also presented.

2. The Electronic Structure of the Cu_2 Center

The intensity of the MCD signals shown in Figure 3 a are temperature and magnetic-field dependent (contribution of the MCD C-term) and increases with lower temperature and higher magnetic field. The MCD intensity will eventually saturate at high field ($\approx 7 \text{ T}$) and low temperature ($\approx 2 \text{ K}$). Different spin-state systems have different saturation behaviors.^[32] Variable temperature, variable field (VTVH) saturation MCD can thus determine the spin state of the resting Cu_2 center, which is the state of the crystallographically defined Cu_2 cluster. The VTVH MCD saturation of resting Cu_2 is shown in Figure 3 b along with theoretically calculated saturation curves for $S = 1/2$, 1, and $3/2$ systems, which show that the resting Cu_2 center has an $S_{\text{total}} = 1/2$ ground state.^[29]

Since the Cu_2 center is a tetranuclear copper cluster, there are two possibilities for the copper oxidation states to give $S_{\text{total}} = 1/2$, either 1 $\text{Cu}^{\text{II}}/3 \text{Cu}^{\text{I}}$ or 3 $\text{Cu}^{\text{II}}/1 \text{Cu}^{\text{I}}$ (Cu^{II} , d^9 , oxidized; Cu^{I} , d^{10} , reduced). In the latter case, two of the oxidized copper atoms would have to be antiferromagnetically coupled. Cu K-edge X-ray absorption spectroscopy (XAS) was used to distinguish between these two possibilities. Cu^{I} complexes have an intense characteristic absorption feature at approximately 8984 eV, which is the electric-dipole-allowed $\text{Cu } 1s \rightarrow 4p$ transition, while Cu^{II} complexes have no intense feature below 8985 eV. Instead they have a very weak transition at about 8979 eV, which is the electric-dipole-forbidden $\text{Cu } 1s \rightarrow 3d$ transition.^[33] The copper K-edge X-ray

absorption spectrum of resting Cu_z is given in Figure 4, along with simulated spectra for the 1 Cu^{II}/3 Cu^I and 3 Cu^{II}/1 Cu^I configurations. The simulations show that the 1 Cu^{II}/3 Cu^I model is far better than the 3 Cu^{II}/1 Cu^I alternative, which

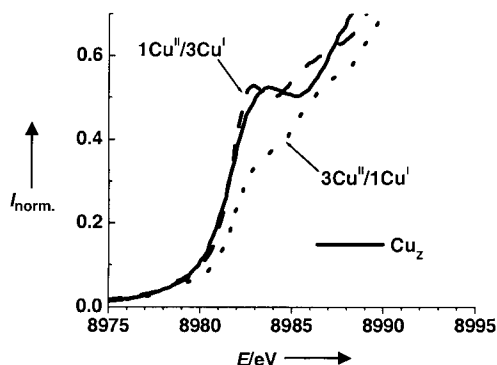


Figure 4. Cu K-edge XAS spectrum of resting Cu_z from *Pn* N₂OR and simulated spectra assuming 1 Cu^{II}/3 Cu^I and 3 Cu^{II}/1 Cu^I oxidation state configurations.

indicates that there is only one oxidized Cu^{II} in the Cu_z cluster with a single spin (a single Cu d-hole).^[29]

EPR spectroscopy was used to determine the distribution of the single spin (from one Cu^{II} center) over the Cu_z center. The Q-band ($\nu \approx 35$ GHz) EPR spectrum of resting Cu_z (Figure 5a) shows an axial pattern with $g_{\parallel} \approx 2.16 > g_{\perp} \approx 2.04 > 2.0$, indicating that the single spin resides in a Cu d_{x²-y²}

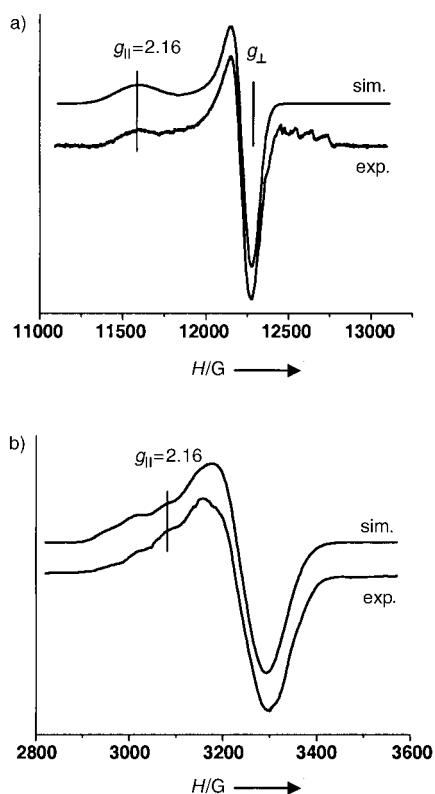


Figure 5. Experimental and simulated EPR spectra of resting Cu_z from *Pn* N₂OR at a) Q-band and b) X-band.

orbital.^[34] The g_{\parallel} value of resting Cu_z is very small as compared to the approximately 2.3–2.4 for normal tetragonal Cu^{II} complexes (e.g. CuSO₄).^[35] This could be due to extensive covalent character in the metal–ligand bonding or high d–d transition energies.^[35] High transition energies affect the g values as the spin-orbit coupling of these excited states with the ground state leads to the g values deviating from 2.0023, and this deviation will decrease as the energies of these excited states increase. In correlating the Q-band to the lower frequency X-band ($\nu \approx 9.3$ GHz) EPR spectrum of resting Cu_z, metal hyperfine coupling is resolved in the g_{\parallel} region (Figure 5b). Mapping the g values determined from the Q-band EPR onto the X-band EPR spectrum, the g_{\parallel} value (≈ 2.16) coincides with a hyperfine feature indicating metal hyperfine pattern with an odd number of lines (Figure 5b). This is in contrast to the EPR hyperfine pattern of normal mononuclear Cu^{II} complexes, which is a four-line pattern (Cu nuclear spin = $\frac{3}{2}$).^[35] To account for the X-band metal hyperfine pattern, two copper centers are required for the hyperfine coupling. One copper center dominates the hyperfine splitting ($A_{\parallel} = 61 \times 10^{-4} \text{ cm}^{-1}$) and a second copper center contributes somewhat less with $A_{\parallel} = 24 \times 10^{-4} \text{ cm}^{-1}$. The ratio of the hyperfine coupling constants gives the approximate ratio of spin densities on the two copper atoms, approximately 5:2. Therefore, resting Cu_z in *Pn* N₂OR can be described as a partially delocalized mix-valent system with the single spin predominantly in a d_{x²-y²} orbital on one copper atom.^[29]

XAS at the Cu K-edge was used to determine the copper oxidation states of resting Cu_z. XAS at the sulfur K-edge (S K-edge) was also used to determine the bridging-sulfide covalency in the ground state of resting Cu_z.^[36] The pre-edge transition at the S K-edge is the S 1s → ground state SOMO transition, where the SOMO is a linear combination of Cu 3d and S 3p orbitals (Figure 6a). The intensity of this pre-edge transition is directly proportional to the sulfide covalency α^2 in the ground-state wave function (see Equation in Figure 6a).^[36] Figure 6b presents the S K-edge spectrum of resting Cu_z,^[37] where the S pre-edge transition occurs at approximately 2469 eV and its weak intensity corresponds to around 15–22% sulfur character in the ground-state wave function. For comparison, the S K-edge spectrum of the Cu_A center (also given in Figure 6b) has a much stronger pre-edge feature at about 2470 eV. The intensity of this Cu_A pre-edge transition corresponds to approximately 46% S character in the ground state, which is well documented.

Density functional theory (DFT) calculations were used to obtain a detailed description of the resting Cu_z ground-state wave function. Figure 7 and Table 1 give the optimized structures and atomic spin densities of the spin-doublet state of the Cu_z cluster with different Cu_I/Cu_{IV}-edge ligands. These calculations indicate that the ground-state wave function and the spin-density distribution of the Cu_z cluster are sensitive to the nature of the ligand at the Cu_I/Cu_{IV} edge. In general, Cu_I is the predominantly oxidized copper center (Table 1). This situation is consistent with Cu_I having a four-coordinate structure and the other copper atoms having lower coordination numbers (see Figures 2 and 7). The spin distribution between the Cu_I and Cu_{II} atoms in the cluster with L = H₂O and the spin distribution between the Cu_I and Cu_{IV} atoms in

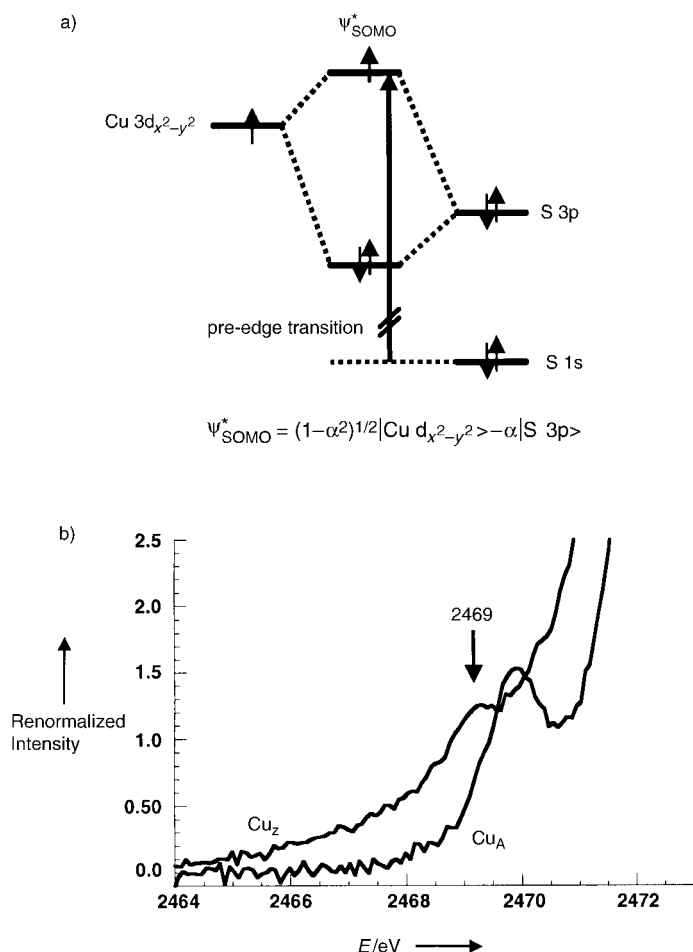


Figure 6. a) Methodology of S K-edge XAS. SOMO: singly occupied molecular orbital. b) Sulfur K-edge spectra of resting Cu_2 from *Achromobacter cycloclastes* N_2OR and Cu_A center.

the cluster with $\text{L} = \text{HO-H-OH}^-$ have an approximately 2:1 ratio. This ratio is in agreement with the Q/X-band EPR results which indicate an approximately 5:2 ratio. The complexes with other water-derived ligands show a spin distribution different from 5:2. This observation suggests H_2O or the HO-H-OH^- ion as the edge ligand in the resting form of the Cu_2 cluster. In these species, the μ_4 -bridging sulfide group contributes around 13–16% to the ground-state wave function, which is also consistent with the S covalency determined from the S K-edge results (Figure 6b). The

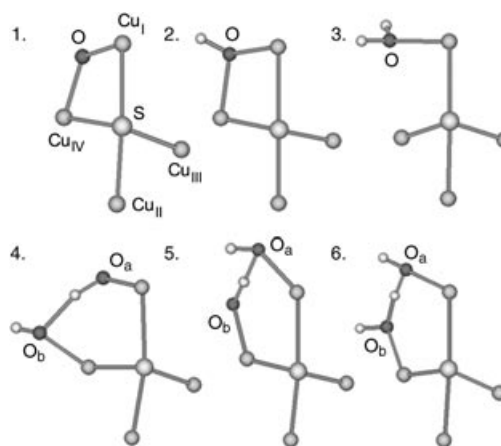


Figure 7. The optimized structures of the Cu_2 cluster with different $\text{Cu}_I/\text{Cu}_{IV}$ edge ligands L from spin unrestricted calculations at the BP86/LanL2DZ level. The Cu_4S core and the ligand L coordinates of Cu_2 were optimized while the histidine ligand (modeled as imidazole, not shown here for clarity) positions were kept frozen to those from the crystal structure of *Pd N2OR*; L ligands: 1) O^{2-} , 2) OH^- , 3) H_2O , 4) and 5) two OH^- , and 6) H_2O and OH^- ; other $\text{L} = \text{H}_3\text{O}_2^-$, $\text{L} = \text{O}_2\text{H}_2^{2-}$ species were considered. These results will be reported elsewhere. The complex with two H_2O ligands was considered as well, however, the calculations showed that such a structure is not stable. O_a and O_b refer to Table 1.

electron delocalization in the Cu_2 cluster is very important because it contributes to a low reorganization energy during redox processes of the Cu_2 center and leads to stabilization of the oxidized form of Cu_2 after N_2O reduction.

The description obtained from the ground-state wave function greatly facilitates the understanding of other characteristic spectroscopic features of resting Cu_2 cluster. Figure 8a presents the resonance Raman spectrum of resting Cu_2 clusters excited at 624.4 nm.^[30] Three dominant features are observed, at 366, 386, and 415 cm^{-1} , all of which shift to lower frequencies upon ^{34}S isotope labeling.^[39] Based on the frequencies and ^{34}S isotope shifts, these three vibrations can be assigned as Cu–S based stretching vibrations. The vibration modes observed can be understood by using a Cu_4S cluster model, which has an approximate C_s symmetry with $\text{Cu}_I\text{-S-Cu}_{II}$ defining the mirror plane (Figure 2).^[25] There are four Cu–S bonds in this cluster and thus a total of four Cu–S based stretching modes: two symmetric (A' symmetry in the C_s point group) in-plane modes from $\text{Cu}_I\text{-S}/\text{Cu}_{II}\text{-S}$ vibrations and two out-of-plane modes, one the symmetric (plus)

Table 1: Atomic spin densities^[a] of the Cu_2 cluster with different ligands on the $\text{Cu}_I/\text{Cu}_{IV}$ edge (see Figure 7 for structures).

Ligand	Ratio ^[b]	Cu_I	Cu_{II}	Cu_{III}	Cu_{IV}	S	O_a	O_b
O^{2-}	5.7 (19)	0.31 (0.40)	0.02 (0.01)	0.01 (0.01)	0.06 (0.02)	0.11 (0.13)	0.48 (0.42)	–
OH^-	3.4 (5.2)	0.41 (0.45)	0.07 (0.08)	0.05 (0.07)	0.12 (0.01)	0.22 (0.26)	0.07 (0.06)	–
H_2O ^[38]	2.4 (2.0)	0.42 (0.39)	0.18 (0.19)	0.07 (0.07)	0.04 (0.05)	0.15 (0.16)	0.01 (0.01)	–
O-H-OH^{2-}	5.1	0.47	0.00	0.01	0.09	0.11	0.28	0.01
HO-H-O^{2-}	1.4	0.24	0.00	0.00	0.34	0.08	0.04	0.28
HO-H-OH^-	1.7 (3.6)	0.41 (0.51)	0.06 (0.06)	0.02 (0.02)	0.24 (0.14)	0.13 (0.11)	0.02 (0.05)	0.04 (0.01)

[a] The calculations were performed for the spin-doublet ground state at the spin unrestricted B3LYP/6-311G** level of theory using the BP86/LANL2DZ and B3LYP/6-311G** optimized structures. The spin densities obtained using the B3LYP/6-311G** optimized structures are shown in parenthesis. [b] Ratio of the atomic spin density between the copper atoms with the largest and second-largest values.

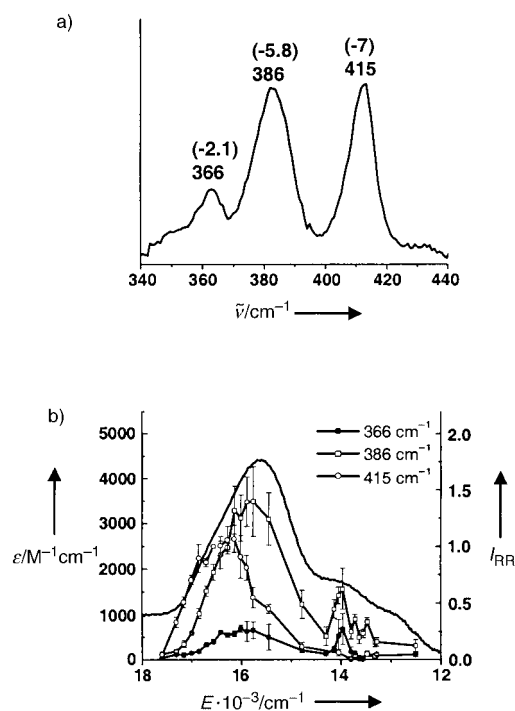


Figure 8. a) Resonance Raman spectrum of resting Cu₂ excited at $\lambda = 624.4$ nm. Numbers in parentheses are ³⁴S isotope shifts. b) Excitation profiles of the resonance Raman (RR) modes (points) of resting Cu₂ overlaid on its low-temperature absorption spectrum (solid line).

combination of Cu_{III}-S/Cu_{IV}-S, and the other the antisymmetric (minus, A' symmetry) combination of Cu_{III}-S/Cu_{IV}-S. The antisymmetric mode should not be resonance enhanced.^[40] Therefore, only three symmetric resonance Raman modes are expected and experimentally observed (Figure 8a). Using the observed vibrational frequencies and ³⁴S isotope shifts, individual Cu-S bond strengths can be determined from a normal coordinate analysis.^[30] The Cu_I-S bond is the strongest (ca. 3.3 mdyn Å⁻¹), the Cu_{II}-S bond is next in strength (ca. 3.1 mdyn Å⁻¹), and the Cu_{III}-S/Cu_{IV}-S bonds are the weakest (ca. 1.3 mdyn Å⁻¹). The bond-strength pattern of the four Cu-S bonds reflects the electronic structure description of the resting Cu₂ site with L = H₂O, where Cu_I is the predominantly oxidized center, Cu_{II} gains some oxidized character through electron delocalization from Cu_I through the bridging sulfide, and Cu_{III} and Cu_{IV} are mostly reduced.

The excitation profiles of the observed resonance Raman modes are shown in Figure 8b, overlaid on the absorption spectrum of resting Cu₂.^[30] All three Cu-S based vibrations are resonance enhanced by excitation in the region of the broad CT absorption envelope centered at approximately 640 nm (≈ 15650 cm⁻¹), which indicates their S → Cu CT nature. Importantly, three individual electronic transitions are resolved in the resonance Raman excitation profiles, at about 14300, 15700, and 16500 cm⁻¹. These three transitions can be associated with excitations from the three p orbitals of the μ_4 -bridging sulfide.

Returning to the absorption and MCD spectra of resting Cu₂, mentioned in the Introduction (Figure 3a), a number of

transitions can be experimentally resolved by a Gaussian analysis of the bands (Figure 9).^[30] The ground-state wave function (spin-down LUMO) is the σ -antibonding combination of mainly the Cu_I d_{x²-y²} and S p_{x'} orbitals and is the acceptor orbital for all the electronic transitions. Three S → Cu CT bands have been identified in the resonance Raman excitation profiles (Figure 8b, and bands 5, 6, 7 in Figure 9). Band 6 is the strongest among the three transitions in the absorption spectrum and can be assigned as the S p_{x'} → spin-down LUMO transition. In this transition, the donor orbital is the direct bonding counterpart to the acceptor orbital and thus this transition has the largest donor-acceptor orbital overlap and is the most intense in the absorption spectrum. Band 5 is the weakest S → Cu CT transition and can be assigned to the transition from the S p_{z'} donor orbital. This S p_{z'} orbital is out of the Cu_I d_{x²-y²} plane and orthogonal to this acceptor orbital (i.e. poor donor-acceptor overlap), which leads to its low intensity in the absorption spectrum. Band 7 is intermediate in intensity in the absorption spectrum and can be assigned to the CT transition out of the S p_{y'} orbital. Since only Cu_I is dominantly oxidized in resting Cu₂, only this center exhibits d-d transitions (Bands 1, 3, 4, and 8, Figure 9).

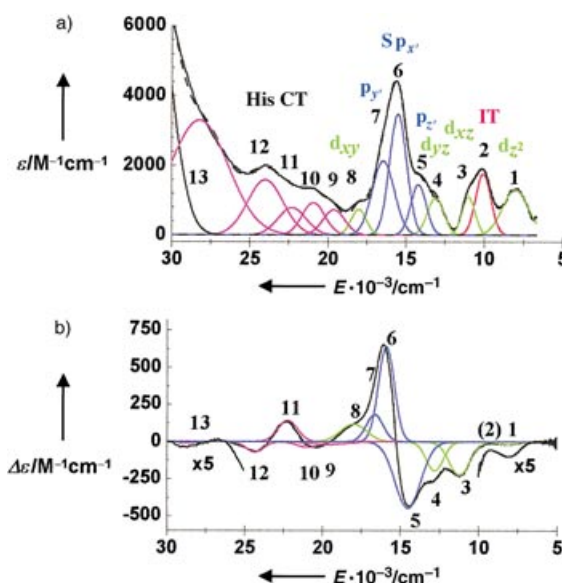


Figure 9. a) 10 K absorption and b) 5 K 7 T MCD spectra of resting Cu₂ with Gaussian-fitting-resolved electronic transitions.

These d-d transitions have a large MCD/absorption intensity ratio, which is due to the large spin-orbit coupling on the copper center ($\xi(\text{Cu}^{\text{II}}) \approx -830$ cm⁻¹).^[41] Interestingly, the d_{xy} → spin-down LUMO transition is high in energy at approximately 18000 cm⁻¹, relative to its position in normal tetragonal Cu^{II} complexes.^[42] Its high energy comes from the ligand geometry of the Cu_I center which has two histidine and one sulfide ligand forming a T-shaped environment with one histidine distorted out of the molecular plane.^[30] The high energy of the d_{xy} transition is the reason for the small g_{||} value (ca. 2.16) observed for the resting Cu₂ cluster, since the covalency of the bridging sulfide is low (ca. 15–22% S char-

acter in the ground state, Figure 6b) and can not account for the observed g_{\parallel} value. Additionally, band 2 in the absorption spectrum of the resting Cu_Z cluster has been identified as an intervalence charge transfer (IT) transition.^[30] This IT transition is unidirectional and thus does not give rise to MCD intensity at low-temperature (Figure 9b).^[43] It formally corresponds to an electron transfer $\text{Cu}^{\text{I}}(\text{d}^{10}) \rightarrow \text{Cu}^{\text{II}}(\text{d}^9)$, and reflects the electronic coupling and electron delocalization between the copper atoms mediated by the bridging sulfide unit. The higher energy bands (9–13, Figure 9) can be assigned as histidine \rightarrow Cu CT transitions. They are in fact low in energy relative to CT transitions in tetragonal copper-imidazole model complexes.^[42] This is due to the low coordination number (three-coordinate) of the Cu_I center in the Cu_Z cluster.

3. Catalytically Relevant State of the Cu_Z Center

Past studies indicate that N_2OR can be activated in vitro to reduce N_2O by incubation with dithionite-reduced methyl viologen, and prolonged pre-incubation can result in higher enzyme activity.^[28,44–47] To identify the catalytically relevant form of Cu_Z , the X-band EPR spectrum of N_2OR was measured after different incubation times in excess methyl viologen and dithionite solution (Figure 10a).^[31] At time zero, the spectrum shows the characteristic EPR signal of resting Cu_Z with $g_{\parallel} = 2.16$. The signal intensity decreases gradually with increasing incubation time. Since resting Cu_Z is at the $1\text{Cu}^{\text{II}}/3\text{Cu}^{\text{I}}$ state with only one electron hole, the loss of the Cu_Z EPR signal in this reducing environment indicates that the Cu_Z cluster is reduced to the 4Cu^{I} form. Parallel activity measurements at similar incubation times show that the enzyme activity increases with increasing incubation time and the increase of activity is directly correlated to the decrease of the resting Cu_Z EPR signal (Figure 10b).^[31] This direct correlation of enzyme activity and reduction of resting Cu_Z indicates that the catalytically relevant form of Cu_Z is the fully reduced 4Cu^{I} state.^[48] Recent measurements using absorption and nitrogen labeling are consistent with these findings.^[49]

4. N_2O Activation and the Role of the Tetranuclear Cu_4S Cluster

Having developed a description of the electronic structure of the resting Cu_Z center and determined the catalytically relevant form of Cu_Z , we could gain insight into the reaction catalyzed by this cluster, which is the two-electron reduction of N_2O to N_2 . The catalytically relevant form of Cu_Z is an electron-rich site with four reduced Cu^{I} centers. At the substrate-binding $\text{Cu}_I/\text{Cu}_{\text{IV}}$ edge (Figure 2), the N_2O substrate could interact with both Cu_I and Cu_{IV} , possibly in a bridged binding mode (Figure 11). Two electrons could be simultaneously donated from Cu_I and Cu_{IV} to overcome the reaction barrier for N_2O reduction. Additionally, there are good electron-transfer pathways from the neighboring Cu_A center in the second subunit of the dimeric N_2OR protein to Cu_{II} and Cu_{IV} .^[29] Together with the delocalized electronic structure of

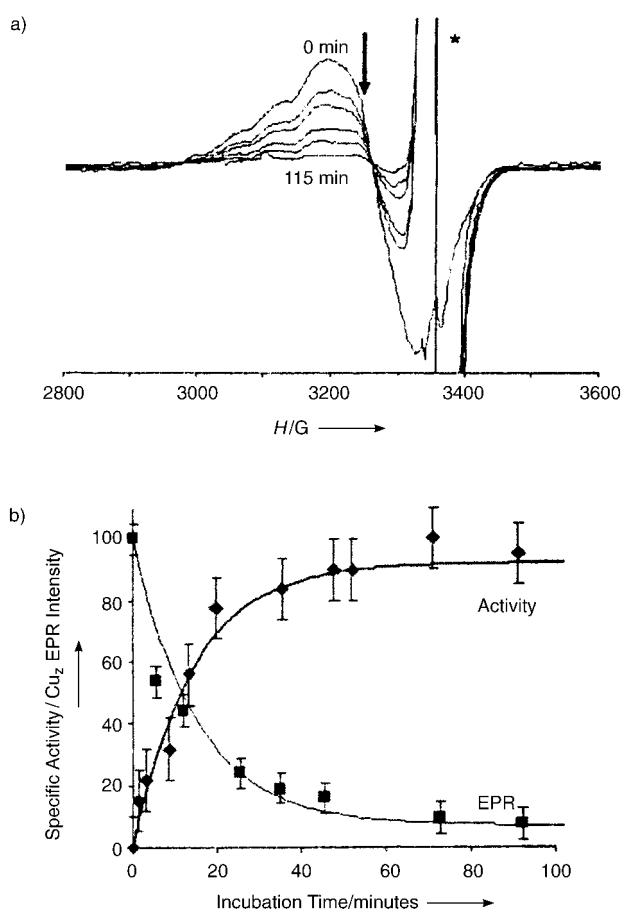


Figure 10. a) Time dependence of Cu_Z EPR signal; * = methyl viologen radical signal. b) Time correlation between PnN_2OR activity (100% corresponds to the reduction of $275 \mu\text{mol N}_2\text{O min}^{-1}$ (mg of enzyme^{-1})) and Cu_Z EPR signal (100% corresponds to the $1\text{Cu}^{\text{II}}/3\text{Cu}^{\text{I}}$ resting form of Cu_Z).

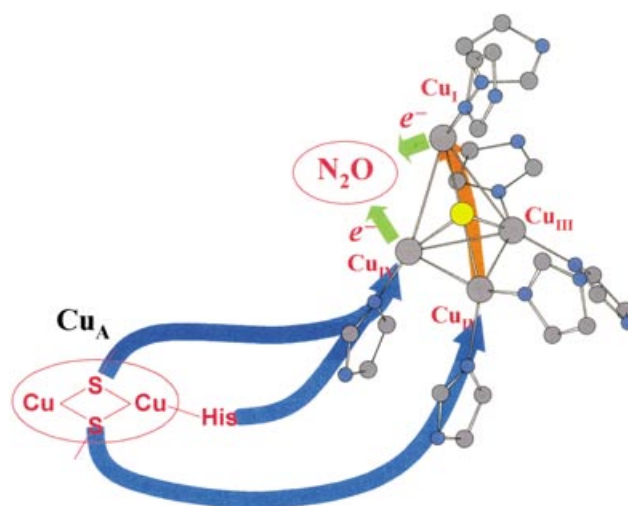


Figure 11. Reduction of N_2O at the Cu_Z site.

the Cu_Z cluster, these could allow rapid re-reduction of the Cu_Z center during enzymatic turnover. The electron delocalization over the bridging sulfide contributes to a low

reorganization energy during redox processes and stabilization of the oxidized form of the Cu_Z center after N₂O reduction.

Computational methods were used to investigate the possible interaction of the N₂O substrate with the catalytic 4Cu^I form of the Cu_Z center.^[31] The lowest energy structure of the Cu_Z(4Cu^I)-N₂O complex is shown in Figure 12, where

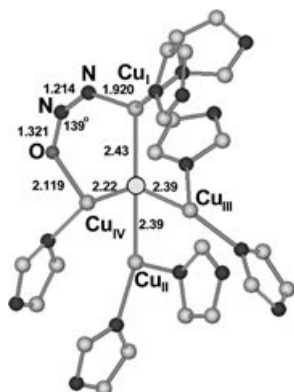


Figure 12. DFT optimized geometry of the N₂O complex with the 4Cu^I form of Cu_Z.^[31]

N₂O binds at the Cu_I/Cu_{IV} edge in a bent μ-1,3 bridging mode (∠N-N-O = 139°) with the terminal nitrogen atom coordinating to Cu_I. (Other binding modes of N₂O to the Cu_Z cluster are higher in energy.) The bending of the bound N₂O unit in the Cu_Z(4Cu^I)-N₂O complex results in a 2 eV splitting of the doubly degenerate LUMO of free N₂O into two nondegenerate π* orbitals. The π* LUMO in the N-N-O plane is stabilized by approximately 3 eV owing to its loss in antibonding character (Figure 13b). This change shifts the π* orbital of N₂O close to the fully occupied d orbitals of the

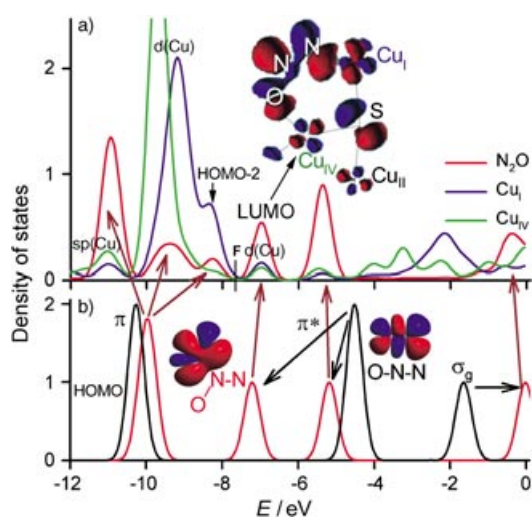
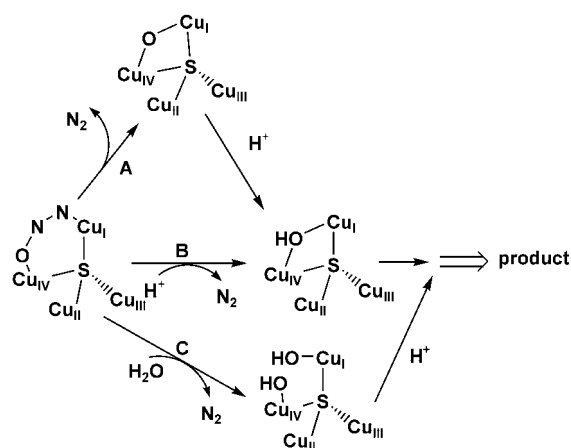


Figure 13. a) Contributions of N₂O, Cu_I, and Cu_{IV} to the density of states of the Cu_Z(4Cu^I)-N₂O complex. The Fermi level is indicated by F. Inset: LUMO of Cu_Z(4Cu^I)-N₂O. b) Density of states of the N₂O molecule with a linear geometry (black line) and with the bent N₂O geometry (red line) in the same Coulomb potential as in the Cu_Z(4Cu^I)-N₂O complex. Inset: the LUMO of bent (left) and linear (right) N₂O.

Cu_Z(4Cu^I) cluster and makes the N₂O ligand a very good electron acceptor.

The LUMO of the Cu_Z(4Cu^I)-N₂O complex (Figure 13 a) has mostly N₂O π* character (54%) with d orbital contributions of 12% from Cu_I and 10% from Cu_{IV}, which indicates significant backbonding interactions from the fully reduced Cu_Z center to the bound N₂O. This substantial Cu_Zd→N₂Oπ* backbonding interaction is reflected in the −0.53 charge of the bound N₂O ligand and the elongation of the N–N and N–O bonds (+0.03 and +0.07 Å, respectively). This strong Cu_Z(4Cu^I)-to-N₂O back donation is only present when N₂O binds at the Cu_I/Cu_{IV} edge in a bent μ-1,3 bridging mode. Other binding modes of N₂O exhibit much weaker back donation (4–5 times smaller).

The electronic interactions between the fully reduced Cu_Z cluster and the bound N₂O ligand play a crucial role in N₂O activation and reduction which leads to N–O bond cleavage. The Cu_Zd→N₂Oπ* backbonding interaction significantly weakens the N–O bond which may facilitate the direct N–O bond cleavage through simultaneous transfer of two electrons from Cu_Z to the μ-1,3 bridged N₂O (Scheme 1



Scheme 1. Possible Channels for N₂O Reduction at the Cu_Z Site.

path A). This backbonding interaction also increases the electron density on the oxygen atom of the bound N₂O molecule (oxygen charge = −0.5), and would activate it for electrophilic attack by a proton (Scheme 1 path B). The HOMO-2 of the Cu_Z(4Cu^I)-N₂O complex, which lies close to HOMO and has significant O character (Figure 13 a), can serve as the donor frontier molecular orbital for protonation. This and other possible reaction channels (Scheme 1 path C) leading to the reductive cleavage of the N–O bond in N₂O are presently being evaluated. Our DFT calculations^[50] indicate that path B is a very favorable reaction channel: oxygen-atom protonation of the coordinated N₂O causes the barrierless N–O bond cleavage.

5. Summary

Spectroscopic methods combined with density functional calculations have been used to define the spin state, copper

oxidation state, spin distribution, and ground-state wave function of the resting Cu_z center, and to understand its unusual vibrational and optical spectral features. The electronic-structure description developed for the resting Cu_z cluster and the determination that the catalytically relevant form of Cu_z is the fully reduced state provide the basis for understanding the role of the μ₄-sulfide bridged tetranuclear copper cluster in the activation of N₂O for two-electron reduction. Strong back donation into the N₂O ligand in the Cu_z(4Cu^I)-N₂O complex where N₂O binds in as bent μ-1,3 bridging mode activates the reductive cleavage of the O–N₂ bond.

Received: December 19, 2003 [M1734]

Published Online: June 30, 2004

- [1] R. A. Sheldon, J. K. Kochi in *Metal-Catalyzed Oxidations of Organic Compounds*, Academic Press, New York, **1981**.
- [2] D. R. Lide, *CRC Handbook of Chemistry and Physics*, 76th ed., CRC, New York, **1996**.
- [3] W. L. Jolly in *The Inorganic Chemistry of Nitrogen*, Benjamin, New York, **1964**.
- [4] F. Bottomley, I. J. B. Lin, M. Mukaida, *J. Am. Chem. Soc.* **1980**, *102*, 5238.
- [5] G. A. Vaughan, G. L. Hillhouse, R. T. Lum, S. L. Buchwald, A. L. Rheingold, *J. Am. Chem. Soc.* **1988**, *110*, 7215.
- [6] G. A. Vaughan, P. B. Rupert, G. L. Hillhouse, *J. Am. Chem. Soc.* **1987**, *109*, 5538.
- [7] P. T. Matsunaga, G. L. Hillhouse, *J. Am. Chem. Soc.* **1993**, *115*, 2075.
- [8] F. Bottomley, J. Darkwa, *J. Chem. Soc. Dalton Trans.* **1983**, 399.
- [9] J. N. Armor, H. Taube, *J. Am. Chem. Soc.* **1969**, *91*, 6874.
- [10] J. T. Groves, J. S. Roman, *J. Am. Chem. Soc.* **1995**, *117*, 5594.
- [11] M. R. Smith, III., P. T. Matsunaga, R. A. Anderson, *J. Am. Chem. Soc.* **1993**, *115*, 7049.
- [12] K. Koo, G. L. Hillhouse, A. L. Rheingold, *Organometallics* **1995**, *14*, 456.
- [13] F. Bottomley, W. V. F. Brooks, *Inorg. Chem.* **1976**, *15*, 501.
- [14] J. N. Armor, H. Taube, *Chem. Commun.* **1971**, 287.
- [15] A. Zecchina, L. Cerruti, E. Borello, *J. Catal.* **1972**, *25*, 55.
- [16] W. G. Zumft, *Microbiol. Mol. Biol. Rev.* **1997**, *61*, 533.
- [17] W. G. Zumft, P. M. H. Kroneck in *Mechanisms of Metallocenter Assembly* (Eds.: R. P. Hausinger, G. L. Eichhorn, L. G. Marzilli), Wiley-VCH, Weinheim, **1996**, p. 193.
- [18] F. Neese, Ph.D. thesis, Universität Konstanz, **1996**.
- [19] F. Neese, W. G. Zumft, W. E. Antholine, P. M. H. Kroneck, *J. Am. Chem. Soc.* **1996**, *118*, 8692.
- [20] D. R. Gamelin, D. W. Randall, M. T. Hay, R. P. Houser, T. C. Mulder, G. W. Canters, S. D. Vries, W. B. Tolman, Y. Lu, E. I. Solomon, *J. Am. Chem. Soc.* **1998**, *120*, 5246.
- [21] J. A. Farrar, A. J. Thomson, M. R. Cheesman, D. M. Dooley, W. G. Zumft, *FEBS Lett.* **1991**, *294*, 11.
- [22] J. A. Farrar, W. G. Zumft, A. J. Thomson, *Proc. Natl. Acad. Sci. USA* **1998**, *95*, 9891.
- [23] K. Brown, M. Tegoni, M. Prudencio, A. S. Pereira, S. Besson, J. J. Moura, I. Moura, C. Cambillau, *Nat. Struct. Biol.* **2000**, *7*, 191.
- [24] T. Rasmussen, B. C. Berks, J. Sanders-Loehr, D. M. Dooley, W. G. Zumft, A. J. Thomson, *Biochemistry* **2000**, *39*, 12753.
- [25] K. Brown, K. Djinovic-Carugo, T. Haltia, I. Cabrito, M. Saraste, J. J. G. Moura, I. Moura, M. Tegoni, C. Cambillau, *J. Biol. Chem.* **2000**, *275*, 41133.
- [26] T. Haltia, K. Brown, M. Tegoni, C. Cambillau, M. Saraste, K. Mattila, K. Djinovic-Carugo, *Biochem. J.* **2003**, *369*, 77.
- [27] Resting Cu_z was prepared by treating the isolated N₂O_R enzyme with excess dithionite solution, the Cu_A center in the enzyme is thus reduced to the spectroscopically silent Cu^I/Cu^I state and does not contribute to absorption, MCD, and EPR signals. See refs. [28,30].
- [28] M. Prudencio, A. S. Pereira, P. Tavares, S. Besson, I. Cabrito, K. Brown, B. Samyn, B. Devreese, J. VanBeeumen, F. Rusnak, G. Fauque, J. J. G. Moura, M. Tegoni, C. Cambillau, I. Moura, *Biochemistry* **2000**, *39*, 3899.
- [29] P. Chen, S. D. George, I. Cabrito, W. E. Antholine, J. J. G. Moura, I. Moura, B. Hedman, K. O. Hodgson, E. I. Solomon, *J. Am. Chem. Soc.* **2002**, *124*, 744.
- [30] P. Chen, I. Cabrito, J. J. G. Moura, I. Moura, E. I. Solomon, *J. Am. Chem. Soc.* **2002**, *124*, 10497.
- [31] S. Ghosh, S. I. Gorelsky, P. Chen, I. Cabrito, J. J. G. Moura, I. Moura, E. I. Solomon, *J. Am. Chem. Soc.* **2003**, *125*, 15708.
- [32] F. Neese, E. I. Solomon, *Inorg. Chem.* **1999**, *38*, 1847.
- [33] L. S. Kau, D. J. Spira-Solomon, J. E. Penner-Hahn, K. O. Hodgson, E. I. Solomon, *J. Am. Chem. Soc.* **1987**, *109*, 6433.
- [34] E. I. Solomon, *Comments Inorg. Chem.* **1984**, *3*, 227.
- [35] B. R. McGarvey in *Transition Metal Chemistry, Vol. 3* (Ed.: R. L. Carlin), Dekker, New York, **1966**, p. 89.
- [36] F. Neese, B. Hedman, K. O. Hodgson, E. I. Solomon, *Inorg. Chem.* **1999**, *38*, 4854.
- [37] S. Debeer George, S. Ghosh, S. I. Gorelsky, J. M. Chan, D. M. Dooley, E. I. Solomon, unpublished results.
- [38] Previous calculations of Cu_z with L = H₂O were performed on a simplified model where the histidine ligands were modeled as NH₃ (see refs. [29,30]). The results for the L = H₂O species presented here are similar to the previous values.
- [39] M. L. Alvarez, J. Y. Ai, W. Zumft, J. Sanders-Loehr, D. M. Dooley, *J. Am. Chem. Soc.* **2001**, *123*, 576.
- [40] R. S. Czernuszewicz, T. G. Spiro in *Inorganic Electronic Structure and Spectroscopy, Vol. 1* (Eds.: E. I. Solomon, A. B. P. Lever), Wiley, New York, **1999**, p. 353.
- [41] A. A. Gewirth, E. I. Solomon, *J. Am. Chem. Soc.* **1988**, *110*, 3811.
- [42] A. B. P. Lever in *Inorganic Electronic Spectroscopy* (2nd ed.), Elsevier, Amsterdam, **1984**.
- [43] E. I. Solomon, E. G. Pavel, K. E. Loeb, C. Campochiaro, *Coord. Chem. Rev.* **1995**, *144*, 369.
- [44] S. Ferretti, J. G. Grossmann, S. S. Hasnain, R. R. Eady, B. E. Smith, *Eur. J. Biochem.* **1999**, *259*, 651.
- [45] J. K. Kristjansson, T. C. Hollocher, *J. Biol. Chem.* **1980**, *255*, 704.
- [46] S. W. Snyder, T. C. Hollocher, *J. Biol. Chem.* **1987**, *262*, 6515.
- [47] B. C. Berks, D. Baratta, D. J. Richardson, S. J. Ferguson, *Eur. J. Biochem.* **1993**, *212*, 467.
- [48] Note that the slow rate of reduction of the resting Cu_z center (1 Cu^{II}/3 Cu^I) indicates that this species can not take part in the catalytic cycle, and the rate of re-reduction of the N₂O-oxidized Cu_z center must be fast in enzymatic turnover.
- [49] J. M. Chan, J. A. Bollinger, C. L. Grewell, D. M. Dooley, *J. Am. Chem. Soc.* **2004**, *126*, 3030.
- [50] S. I. Gorelsky, S. Ghosh, E. I. Solomon, unpublished results.